RESPUESTA LOCAL DEL SITIO EN SAN SALVADOR, EL SALVADOR BASADA EN EL TERREMOTO DEL 10 DE OCTUBRE DE 1986

Kuvvet Atakan[1] y Rodolfo Torres[2]

(1) Instituto de Física de la Tierra Sólida, Universidad de Bergen, Bergen, Noruega.
(2) Centro de Investigaciones Geotécnicas, San Salvador El Salvador, C.A.

RESUMEN

El área de San Salvador está ubicada a lo largo del actual eje de la cadena volcánica centroamericana, que es producto de la subducción de la placa Cocos bajo la placa Caribe con dirección noreste. Los terremotos destructivos ocurridos en El Salvador durante las últimas décadas han sido sismos someros y de tamaño moderado con epicentros ubicados en la cadena volcánica. El más reciente de éstos, el del 10 de Octubre de 1986 (M_S =5.4) ha causado un daño considerable a la ciudad de San Salvador con más de 1500 muertos y alrededor de 10000 lesionados. Las pérdidas materiales alcanzaron los 1.5 billones de dólares americanos. Un código de diseño sísmico es necesitado urgentemente, que tome en cuenta factores cruciales tales como la respuesta local del sitio. El presente estudio pretende demostrar este efecto para proveer una base para los esfuerzos que se están haciendo en preparar el nuevo código de diseño sísmico para El Salvador.

Registros de movimiento fuerte del sismo del 10 de Octubre de 1986 son usados para investigar la respuesta local del sitio en San Salvador. Los cocientes espectrales de las componentes horizontales de cinco sitios sedimentarios con respecto a un sitio de referencia, indican amplificaciones máximas por un factor de 8 - 22. Las amplificaciones varían en diferentes sitios, dependiendo mayormente de las frecuencias. La comparación de resultados mostró que hay al menos 5 picos comunes observados en los cocientes espectrales de todos los sitios a 0.4, 0.7, 1.3, 2.0, y 3.0 Hz. Las amplificaciones más prominentes son encontradas a frecuencias menores de 3.0 Hz. A frecuencias más altas, el fenómeno se invierte dando amplificaciones negativas. Hay generalmente una buena correlación entre el tipo de sedimento y las amplificaciones. Sin embargo, el espesor de los sedimentos no consolidados parece jugar un papel más crítico que el tipo de formación. El mismo grupo de datos es también usado para comparar el método recientemente propuesto de usar cocientes espectrales del mismo sitio, con el objetivo de evaluar su factibilidad, para el cual nuestros resultados no dan ninguna evidencia clara de correlaciones positivas cuando son comparados con el primer método, donde son usados los cocientes espectrales de sedimento contra roca. El uso del método de dos componentes para una misma estación, para estimar la respuesta local del sitio, no es recomendable para el área de San Salvador. Por lo tanto, los resultados obtenidos de relaciones espectrales de sedimento vrs. roca, son más aceptables.

LOCAL SITE RESPONSE IN SAN SALVADOR, EL SALVADOR BASED ON THE OCTOBER 10, 1986 EARTHQUAKE

Kuvvet Atakan[1] and Rodolfo Torres[2]

(1) *Institute of Solid Earth Physics, University of Bergen, Bergen, Norway.*
(2) *Centro de Investigaciones Geotécnicas, San Salvador, El Salvador, C.A.*

ABSTRACT

The San Salvador area lies along the present axis of the Central American volcanic chain, which is the product of the northeast-directed subduction of the Cocos plate beneath the Caribbean plate. The destructive earthquakes occurred in El Salvador during the last few decades, originate basically from shallow, moderate sized earthquakes with epicenters falling into the volcanic zone. The most recent one of these, the Oct.10, 1986 earthquake (M_S=5.4) caused a considerable damage to the city of San Salvador with more than 1500 casualties and about 10,000 injured. The material losses reached up to USD 1,5 billion. An improved seismic design code, is urgently needed, especially taking into account the crucial factors such as the local site response. Present study intends to demonstrate this effect to provide a basis for the ungoing efforts in preparing the new seismic design code for El Salvador.

Strong motion records from the Oct.10, 1986 earthquake are used to investigate the local site response in San Salvador. Spectral ratios of the horizontal components from five sedimentary sites with respect to a reference site, indicate maximum amplifications by a factor of 8-22. The amplifications vary at different sites, largely depending on the frequencies. Comparison of the results showed that there are at least 5 common peaks observed on the spectral ratios of all sites, at 0.4, 0.7, 1.3, 2.0 and 3.0 Hz. The most prominent amplifications are usually found at frequencies lower than 3.0 Hz. At higher frequencies, the phenomena is reversed giving negative amplifications. There is generally a good correlation between the type of the sediment and the amplifications. However, the thickness of the unconsolidated sediments seems to play a more critical role than the type of formation. Same data set is also used comparing the recently proposed method of using spectral ratios from the same site, with the objective of testing its feasibility. Our results do not give any clear evidence for positive correlations when compared to the first method, where the spectral ratios of sediment vs. bedrock are used. Using this latter technique in estimating the local site response is therefore not recommended for the San Salvador area. Instead, the results from the spectral ratios of sediment vs. bedrock, are more applicable.

INTRODUCTION:

Any reliable estimation of seismic hazard, is largely dependent on the detailed information of the local site response. This phenomenon has been recognized for some time *(e.g. Milne, 1898)*. In order to determine the site response, several methods are used, that can be categorized into two major groups, the theoretical (analytical) and the empirical methods. The theoretical calculation of the site response, mainly based on the inversion techniques, basically require a very good knowledge of the geotechnical parameters to constrain the results. Depending on the type of inversion used, several assumptions have to be made regarding the shape of the source spectrum or the site response at the selected stations. Empirical methods are somehow more effective in the sense that they are based on calculating the frequency spectrum directly from the recorded ground motion. Among the empirical methods, the spectral ratio of a sedimentary site with respect to a bedrock reference site is becoming widely used in recent years *(e.g. Borcherdt, 1970; Borcherdt and Gibbs, 1976; Rogers et al., 1984)*. Effective use of this technique is demonstrated at different sites and geological conditions following the large destructive earthquakes during the last decade *(e.g. Singh et al., 1988; Lermo et al., 1988; Borcherdt et al., 1989; Hough et al., 1990)*. Some review papers, discuss the effectiveness of the different methods used in the site response estimate *(e.g. Aki, 1988; Hartzell, 1992; Aki, 1993)*. Some new methods were also introduced recently, based on using only one-station recordings (horizontal vs. vertical components) *(Nakamura, 1989; Lermo and Chávez-García, in press)*, and on the cross-spectrum estimate *(Şafak, 1991; Field et al., 1992)*.

The destructive earthquakes experienced in El Salvador during the last few decades, originate basically from the shallow, moderate sized earthquakes with epicenters falling in to the volcanic zone. The most recent one of these, the Oct.10, 1986 earthquake (M_S=5.4) has caused a considerable damage to the city of San Salvador with more than 1500 casualties and about 10,000 injured *(Olson, 1987)*. The material losses reached up to USD 1,5 billion. An improved seismic design code, is urgently needed, especially taking into account the crucial factors such as the local site response. Present study intends to demonstrate this effect

to provide a basis for the ungoing efforts in preparing the new seismic design code for El Salvador.

In this study, we have used the strong motion records of the Oct.10, 1986 earthquake from the six accelerograph stations located within the metropolitan area of San Salvador, El Salvador *(Figure 1)*. One of the stations (SHE) is located close to the San Salvador volcano, and is used as a bedrock reference site. Spectral ratio method is used to obtain the amplifications at five different sites, related to the different unconsolidated sediments covering most of the metropolitan area. Results are compared with the site responses obtained from another method recently proposed *(Nakamura, 1989)*, using the recordings from one-station, with the objective of testing the feasibility of this method in estimating the site response.

GEOLOGICAL SETTING:

The San Salvador area lies along the present axis of the Central American volcanic chain, which is the product of the northeast-directed subduction of the Cocos plate beneath the Caribbean plate with an absolute plate motion of 8.0 cm/year *(Rymer, 1987; Weinberg, 1992)*. The plate-tectonic framework of the Central America and the Caribbean is previously reviewed by several authors *(e.g. Molnar and Sykes, 1969; Malfait and Dinkelmann, 1972; Burke et al., 1984; Mann and Burke, 1984; Dengo, 1985)*. The generalized geological overview of El Salvador was discussed by Wiesemann *(1975)*, and later the geological map was published by Weber et al. *(1978)*.

The metropolitan area of San Salvador is underlain by middle and upper Cenozoic volcanic and volcanoclastic deposits of different origin, mainly derived from the adjacent volcanoes *(Weber et al., 1978)*. The area lies on the gentle eastern slope of the San Salvador volcano dissected by deeply incised streams and rivers *(Figure 2a)*, and is surrounded by four major volcanic features. These are; the San Salvador volcano, with a minor cinder cone in its center to the west-northwest; the Cerros de Mariona to the north; a collapsed caldera, lake

Ilopango to the east; and an inactive volcanic dome with a minor parasitic cone, Cerro San Jacinto to the south-southeast *(Figure 4)*.

Relevant to the local site response, there are two major deposits forming part of the San Salvador Formation that cover the metropolitan area. These are the youngest unit, Holocene volcanic ashes, locally named as tierra blanca because of its light colour, and the underlying Pleiostecene aged, browned coloured tuffs *(Scmidt-Thomé, 1975)*. The latter unit is as thick as 25 m and is derived from the San Salvador volcano, whereas the younger unit, is approximately 25 m thick immediately underneath the city and may reach up to 50 m towards the lake Ilopango *(Rymer, 1987)*. This younger unit represents multiple eruptions from the former Ilopango volcano. The characteristics of the uppermost 10 to 30 m of these sediments, are revealed in either geotechnical investigations or in cross sections outcropping along the river banks. The clast compositions and the grain sizes vary considerably within short distances as well as the thicknesses. The degree of consolidation is another characteristic feature varying considerably as indicated by the penetration tests *(Figure 2b)*.

There are three major fault trends in the area, in NNE-SSW/N-S, NE-SW and NW-SE *(Durr et al., 1960)*. In addition, the fourth and the oldest trend can be inferred from the general strike direction of the volcanic chain in the WNW-ESE/E-W direction *(Rymer, 1987)*. Among the other three, the north-south trending faults are less distinct and occur only locally *(Rymer, 1987)*. The youngest faults are the dominant trend in the NE-SW and the conjugate set in the NW-SE directions. All faults seem to have steep dip angles generally larger than 65° and appear active *(Schmidt-Thomé, 1975)*. Although the individual fault trends may have developed at different times, they have been repeatedly reactivated. The reactivation of the NNE-SSW trending fault during the October 10, 1986 earthquake is the most recent example.

SEISMICITY:

In El Salvador, as well as in most Central American countries, the main cause of seismic activity is the subduction of the Cocos plate under the Caribbean plate with an average velocity of 8 cm/yr *(Weinberg, 1992)*. Around 80% of the seismic activity in El

Salvador has its origin in the subduction zone. The other 20% is generated either by local fault movements or volcanic activity.

The city of San Salvador has experienced several destructive earthquakes within this century. The most damaging were; on June 8, 1917, where two almost consecutive events with magnitudes 6.4 and 6.3 (M_S) occurred respectively, followed by an eruption half an hour later; on April 27, 1919 (M_S=6.0); and on May 3, 1965 (M_S=6.0), where it was preceeded by an unusual number of shocks (more than 8000) *(White et al., 1987)*. Although the epicenter of the latter is close to the October 10, 1986 earthquake, the casualties were much lower due to the high number of foreshocks which alerted the population. Even though the earthquakes ocurring in the subduction zone have larger magnitudes than the ones occurring inland they are less destructive. This is mainly due to the relative larger epicentral distances and deeper focal depths. As in the case of El Salvador, the most destructive earthquakes in Central America have been inland earthquakes related to the volcanic zone. Among them, December 23, 1972 earthquake in Nicaragua (M_S=6.2; NEIS), April 14, 1973 in Costa Rica (M_S=6.5; NEIS), February 4,1976 in Guatemala (M_S=7.5; NEIS) and October 10, 1986 in El Salvador (M_S=5.4; NEIC) have caused considerable damage and a high number of casualties.

The earthquake of Oct.10, 1986:

Practically no earthquakes preceded the October 10, 1986 earthquake, only one event (M_C=3.8), on July 18 and three aftershocks were located near the epicenter of the main shock. However, this type of seismicity is commonly recorded along the volcanic chain in El Salvador.

The main shock occurred at 17:49 (UT) with an epicenter close to the southern end of the city of San Salvador (Latitude 13° 40' N; Longitude 89° 11.4' W; Depth=7.3km) *(White et al., 1987)*. Despite its relatively moderate magnitude (M_S=5.4; mb=5.1; M_W=5.6), this earthquake caused more than 1500 casualties and left more than USD 1.5 billion in material losses.

The two largest aftershocks occurred in the northern and western part of the city, the first, 14 minutes after the main shock on October 10 (M_C=4.8), and the second on October 13, at 22:24 (M_C=4.6), respectively *(Figure 4)*. Within the next 24 hours following the mainshock, a total of 790 events were recorded *(Alvarez, 1987)*. The activity lasted until May 1987, decreasing sharply after the first three months. The distribution of the majority of the aftershock epicenters until October 13, indicates a clear trend propagating in the NNE direction. This zone was expanded during the period from October 18, to October 25, with still the majority of the aftershocks occurring in the NNE direction. The depth distribution indicates a range from the surface to 15 km, with a concentration around 5-11 km *(White et al., 1987)*. The fault plane solution of the main shock, based on the first motions and on the aftershock distribution, indicates a left-lateral strike slip displacement along a plane striking N32°E dipping nearly vertical *(Figure 4)* (NP1: ϕ 122°, δ 90°, 168°; NP2: ϕ 212°, δ 78°, 0°) *(White et al., 1987)*.

The main shock of the October 10, 1986 earthquake reached intensities as high as IX on the Modified Mercalli intensity scale mainly in the area along the fault plane striking NNE-SSW *(Alvarez, 1987) (Figure 3)*. The highest intensities also correspond to the central and densely populated part of the city. *Figure 3* shows the distribution of damage with increasing degree of intensity, as well as the macroseismic intensity contours. The shallow depth of the mainshock has resulted in high damage concentrated in a relatively narrow zone. This, combined with the fact that most of the damage to buildings was the result of poor construction practices, have lead to a large number of casualties reaching up to 1500 with more than 10,000 wounded *(Olson, 1987)*.

When the October 10, 1986 earthquake occurred, 11 high-gain telemetered seismograph stations and 4 low-gain stations were operating. There was also a strong motion network composed of 10 three component accelerographs located in and around the city of San Salvador. The six accelerograph stations, Centro de Investigaciones Geotécnicas (CIG), Instituto Geográfico Nacional (IGN), Instituto Vivienda Urbana (IVU), Universidad Centro Americana (UCA), Hotel Camino Real (HCR) and Hotel Sheraton (SHE), used in this study are shown in *Figure 1*. Table I summarizes the location of these stations and the epicentral distances to the mainshock.

SPECTRAS AND THE SPECTRAL RATIOS:

Sediment vs. bedrock:

The spectral ratios of the five sedimentary sites CIG, IGN, IVU, UCA and HCR are computed with respect to the bedrock reference site SHE. The S-wave window, including the S-wave coda (believed to give similar amplifications *e.g. Gutierrez and Singh, in press)*, recorded on N-S and E-W components, are selected to study the spectral amplification. The signals were cosine-tapered and Fourier transformed. The spectral amplitudes were then smoothed with one-third octave band filter.

The SHE station is underlain by Pleistocene basaltic and andesitic lavas originating from the San Salvador volcano *(Figure 2a)*. The sedimentary cover, the browned coloured tuff, is less than 3 m thick *(Centro de Investigaciones Geotécnicas, 1987)*. This geological information, together with the low maximum observed absolute accelerations at SHE with respect to other sites, *(Table I, see also Figure 1)*, have allowed us to assume reasonably that SHE can be used as a bedrock reference site. This is also supported by the comparisons obtained using the spectral ratios of horizontal vs vertical components from the same site, where SHE showed very little amplifications. The amplification related to the SHE site, which is by a factor of 2, is later taken into consideration within the relevant frequency range, when comparing the site amplifications from the different sites.

Regarding the location of the earthquake source, we assume that the path effects due to the differences in the geographical locations of the sites, are minimal. In order to adress to the possible effects related to source and wave propagation paths, we have generated synthetic accelerograms for the six stations used in the study, using Herrmann's code *(Herrmann, 1985)*. The station locations, distances and azimuths are given in *Table I*. The crustal model used is the one shown in *Table V*. The focal mechanism is from *White et al. (1987)*. The relative comparison of the accelerograms indicate that the observed differences in the S-wave amplitudes (i.e. giving higher amplifications on the sedimentary sites with respect to the reference site at SHE), are not the results of combined source and path effects.

The comparison shown in *Figure 11* between the sites SHE, CIG and IGN, indicates in fact an opposite effect on the synthetic accelerograms (i.e. higher amplitudes on SHE when compared to CIG and IGN). The observed traces can therefore be compared to analyse the site amplifications.

Several general observations are made on the spectras and the spectral ratios of the N-S components *(Figure 5)*. Generally all sedimentary sites have higher spectral amplitudes than the reference site within the frequency range 0.1 to 3.5. The different frequency ranges on which the positive site amplifications observed are summarized in *Table III*. The situation is reversed at higher frequencies giving negative amplifications at the sedimentary sites. The site amplifications vary from a factor of 8 to 22 *(Figure 7b; see also Table II)*. The highest site amplification is observed at IGN by a factor of 22. There are at least five critical frequencies on which the peak amplifications occur on the spectral ratios. These are, at 0.4, 0.7, 1.3, 2.0, and 3.0 Hz. These peaks are common at all sites. The amount of amplifications are largely frequency dependent and vary at different sites. However, in general the most prominent peaks are observed at either 0.7 or 1.3 Hz *(Figure 8a; see also Table IV)*.

The E-W components give also similar results, although there are some differences in the frequency ranges on which the amplifications occur *(Figure 6; see also Table III)*. There seems to be no amplifications at HCR with respect to SHE. At CIG the positive amplifications continue also at higher frequencies up to 10 Hz. IGN, IVU and UCA, on the other hand, have similar frequency ranges with slightly lower limits. In general the amplifications on the E-W components are lower than the N-S components and range from a factor of 2 to 8. The highest amplification is observed at IVU *(Figure 7c; see also Table II)*. Similar to N-S components, the amplifications are largely dependent on the frequencies *(Figure 8b; see also Table IV)*. Same five critical frequencies are also observed on the E-W components *(Figure 6)*.

Horizontal vs. vertical components:

The site response based on only one-station recordings has recently been suggested by Nakamura *(1989)* and is succesfully applied to a case in Mexico *(Lermo and Chávez-*

García, in press). It is assumed that the spectral ratios of the horizontal components with respect to the vertical, give an estimate of site response. The method is quite attractive since it eliminates the problem of having a recording bedrock reference site, which is usually the case, especially for the earlier records. We have used this method on four of the sedimentary sites at CIG, IGN, UCA and HCR, with the objective of comparing the results from the standard spectral ratio method and testing its feasibility. In addition, SHE is also used to see the effect of the site amplifications (if any), related to that site. The vertical record from IVU is missing and therefore not included in the analysis.

Both N-S and the E-W components vs vertical for the five sites mentioned, give different results than expected *(Figures 9 and 10)*. The only site, where there is a better correlation with the previous method is at IGN. However, the amplification factors are somewhat lower than the estimates obtained by the previous method. The critical frequencies at 0.4, 0.7, and 1.3 seem to be present, whereas no peaks observed at 2.0 and 3.0 Hz.

DISCUSSION:

Several observations related to the comparison of the spectral amplifications at different sites are open to discussion. To provide a basis for these comparisons, some 3-D diagrams are prepared showing the differences between the five sedimentary sites, and are presented in *Figures 7 and 8*. These are only prepared for the results from the first method using the spectral ratios of the five sedimentary sites with respect to the bedrock reference site, basically because this method seems to be more reliable than the method of using only one station recordings.

Regarding the comparison between the maximum and the average (being the average of all amplifications at equal intervals within the frequency range where spectral amplifications occur) spectral amplifications, the N-S components give larger amplifications at all sites *(Figure 7)*. The site IGN, gives the highest amplification factor (x22), whereas the three sites CIG, IVU and HCR have also relatively high amplifications, 15, 14 and 17, respectively *(Table II)*. The UCA site, gives the lowest amplification close to a factor of 8. The average

values between 3 and 6, give similar relative comparison between the sites. The same is also true for the E-W components, except HCR, where the average value is much lower than expected *(Figure 7)*. It is important to note here, that there is no good correlation between the highest absolute accelerations and the maximum amplification factors *(Figure 7)*. The highest absolute acceleration for the N-S components is observed at IVU, whereas the highest amplification factor is at IGN. The comparisons shown in *Figure 8*, clearly demonstrate the frequency dependency of the spectral amplifications. In general 0.7 and 1.3 Hz seem to give the highest amplifications at most of the sites. There is also a tendency of decreasing amplifications with increasing frequencies *(Figure 8; see also Table IV)*.

Based on the above considerations, we have tried to do some corelations with the spectral amplifications and the local geology. In general, the thickness of the sedimentary cover seems to be a more crucial factor than the type of formation. The example to be given here are from the sites which have similar compositions but different thicknesses. In this respect IGN and UCA, having the same composition, which is Pleistocene aged, browned colored tuff, usually stratified with volcanic ash, can be compared *(Figure 2a)*. The geographical locations suggest that the IGN station has a larger thickness and thereby gives larger site amplifications. Regarding the spectral shapes and the dominant peaks in the spectral ratios, both sites give similar results *(Figure 5)*. Similarly, comparison between the sites IVU and HCR is done. They both have similar compositions (Holocene volcanic ash/tierra blanca) and similar topographical levels. The site amplification is higher on HCR with respect to IVU. The site CIG, has a similar formation as the HCR and IVU (Holocene volcanic ash) *(Figure 2a)*. The topographical levels are different suggesting that CIG has a lower topographical level, which is expected to contain thicker sedimentary cover. But, since it is close to the San Jacinto hill, this assumption may not be totally true. Here, the site amplification is slightly lower than the IGN station, but the spectral shapes are very similar *(Figure 5)*.

In the above discussion about the correlation between the sedimentary thicknesses and the spectral amplifications, the degree of consolidation of the sediments (i.e. cementation and compaction), a rather critical factor, must be taken into consideration. There is unfortunately no detailed information available to do a thorough analyses of this problem. However, based

on the geotechnical data available at few of the sites, the degree of consolidation seems to play an important role in the spectral amplifications. An example can be given, comparing the two sites UCA and HCR. HCR gives higher spectral amplifications than UCA, although the thickness of the total sedimentary cover at UCA is higher than HCR (i.e. approximately 33 m at UCA and 21 m at HCR; *Italtekna/Italconsult, 1987*). The thickness of the unconsolidated parts of the sedimentary cover, on the other hand, is opposite being thicker at HCR than UCA, which seems to support the assumption that the degree of consolidation is an important parameter. This problem is generally quite difficult to adress, unless there is a detailed information about the local variations of this parameter. The two cross-sections shown in *Figure 2b* (see variation in the penetration test results at short distances, given at each location), clearly illustrates this problem.

Several recent observations about the weak motion and the strong motion suggest that the non-linear amplification at sediment sites may be very common *(e.g. Singh et al., 1988; Aki, 1993)*. First, on the average, the amplification is always greater at the younger sedimentary sites for all frequencies up to 12 Hz, in the case of weak motion; while the relation is reversed for frequencies higher than 5 Hz, in the case of strong motion *(Aki, 1993)*. Our observations also indicate a reversing of the same relation. However, the frequencies in which the reversing occur are slightly lower than the frequencies mentioned by Aki *(1993)*. At CIG the reversing occurs at 3.8 Hz, at UCA it is at 3.4 Hz, at IGN and HCR it is at 2.3 Hz, and at IVU it is at 3.3 Hz. It has also been argued *(Aki, 1993)* that for the epicentral distances less than 50 km, peak ground velocity and displacement, as well as the Arias intensity, show higher amplifications for soil sites, while peak ground acceleration is roughly independent of the site classification. In our observations on the accelerograms, we observe the site dependent amplifications very clearly. This is in contrast with the previous observations done at other areas *(e.g. Boore et al., 1989)*.

The distribution of damage *(Figure 3)*, and the spectral amplifications at different sites are correlated *(Figure 7)*. There seems to be a positive correlation for the IGN and CIG sites, where clear site amplifications occur close to those parts that have experienced a high damage. The number of sites used in this study, however, are not sufficient to do any detailed comparison between the damage and site amplifications. This comparison becomes

especially difficult, when factors such as the engineering properties for the collapsed structures, vary considerably.

The results from this study clearly demonstrate the site amplifications related to the sedimentary cover in the metropolitan area of San Salvador. It is strongly recommended that the local site response should be taken into consideration in any seismic hazard estimation. The October 10, 1986 earthquake data provides a unique data set to calibrate the site response estimates from any other study. Furthermore, our results from the technique using only one-station recordings for the San Salvador area, do not give any reliable site response estimates. More comprehensive testing at different site conditions is needed, before recommending its use at least in the San Salvador area.

ACKNOWLEDGMENTS:

We thank Enrique Molina, for providing the digitized accelerograph recordings. The geotechnical and the geological information is largely based on the unpublished work by the staff at the Dept. of Geology, Centro de Investigaciones Geotécnicas, El Salvador. Jane K. Ellingsen has kindly helped with the drawings. The computer program, used in calculating the spectral ratios (DEGTRA), is kindly provided by Mario Ordaz. This study was completed while one of the authors, Rodolfo Torres, was visiting scientist at the Institute of Solid Earth Physics, University of Bergen, Norway, sponsored by NORAD.

REFERENCES:

Aki,K. (1988). Local site effects on strong ground motion. Proc. Earthq. Eng. Soil Dyn. II. 103-155.

Aki,K. (1993). Local site effects on weak and strong ground motion. **IN:** F.Lund (Ed.), *New Horizons in Strong Motion: Seismic Studies and Engineering Practice.* Tectonophysics, **218**, 93-111.

Alvarez,S. (1987). Informe técnico-sismológico del terremoto de San Salvador del 10 de Octubre de 1986. (Internal Report) Ministerio de Obras Públicas, Centro de Investigaciones Geotécnicas, Departamento de Sismología, San Salvador, April 1987, 83p.

Boore,D.M., Seekins,L. and Joyner,W.B. (1989). Peak acceleration from the 17 October 1989 Loma Prieta earthquake. Seism. Res. Lett., **60**, 151-166.

Borcherdt,R.D. (1970). Effects of local geology on ground motion near San fransisco Bay. Bull. Seism. Soc. Am. **60**, 29-61.

Borcherdt,R.D., and Gibbs,J.F. (1976). Effects of local geological conditions in the region on ground motions and the intensities of the 1906 earthquakes. Bull. Seism. Soc. Am. **66**, 467-500.

Borcherdt,R.D., Glassmoyer,G., Der Kiureghian,A., and Cranswick,E. (1989). Results and data from seismologic and geologic studies following earthquakes of December 7, 1988 near Spitak, Armenia, S.S.R., U.S.Geol.Surv. Open-File Report, 89-163A.

Burke,K., Cooper,C., Dewey,J.F., Mann,P. and Pindell,J.I. (1984). Carribean Tectonics and relative plate motions, in Caribbean-South-American plate. Mem. Geol. Soc. Am., **162**, 31-63.

Centro de Investigaciones Geotécnicas (1987). Mapa geológico-tectónico del área San Salvador y alrededores. Esc: 1:15 000.

Dengo,G. (1985). Mid-America: Tectonic setting for the Pacific margin from southern Mexico to northwestern Colombia. **IN:** H.E.M.Naim, F.G.Stehli, and S.Uyeda (Eds.), *The Ocean Basins and Margins.* Plenum, New York, 123-180.

Durr,F., et al. (1960). Energía Geotérmica. Informe No.1, Servicio Geológico Nacional, San Salvador, 268p.

Field,E.H., Jacob,K.H., and Hough,S.E. (1992). Earthquake site response estimation: a weak motion case study. Bull. Seism. Soc. Am., **82**, 2283-2307.

Hartzell,S.H. (1992). Site response estimation from earthquake data. Bull. Seism. Soc. Am., **82**, 2303-2327.

Herrmann,R.B. (1985). Computer programs in Earthquake Seismology. Vol.**VI**: Regional Seismograms: Wavenumber Integration. Saint Louis University, Missouri, U.S.A.

Hough,S.E., Borcherdt,R.D., Friberg,P.A., Busby,R., Field,E., and Jacob,K.H. (1990). the role of sediment-induced amplification in the collapse of the Nimitz freeway during the October 17, 1989 Loma Prieta earthquake. Nature **344**, 853-855.

Italtekna/Italconsult (1987). Studi di risposta sismica locale ed elaborazione delle carte di microzonazione sismica. (Unpbl. Report) Consorzio Salvador e San Salvador Programma di Ricostruzione, Republica Italiana, Ministerio Degli Affari Esteri Direzione generale Per La Cooperazione Allo Sviluppo, Parte 4a, 67p.

Lermo,J.F. and Chávez-García,F.J. (in press). Site effect evaluation using spectral ratios with only one station.

Lermo,J., Rodriguez,M., and Singh,S.K. (1988). The Mexico earthquake of September 19, 1985: natural period of sites in the valley of Mexico from microtremor measurements and from strong motion data. Earthquake Spectra **4**, 805-814.

Malfait,B.T., and Dinkelmann,M.G. (1972). Circum-Caribbean tectonic and Igneous activity and the evolution of the Caribbean plate. Geol. Soc. Am. Bull., **83**, 251-271.

Mann,P., and Burke,K. (1984). Neotectonics of the Caribbean, Rev. Geophys., **22**, 309-362.

Milne,J. (1898). Seismology. 1st ed., London, Kegan Paul, Trench, Truber.

Molnar,P., and Sykes,L.R. (1969). Tectonics of the Caribbean and the Middle America regions from focal mechanisms and seismicity. Geol. Soc. Am. Bull., **89**, 1639-1684.

Nakamura,Y. (1989). A method for dynamic characteristics estimation of subsurface using microtremor on the ground surface, QR o RTR1 **30**, 1, February.

Olson,R.A. (1987). The San Salvador earthquake of October 10, 1986: overview and context. Earthquake spectra, Vol.**3**, No.3, 415-435.

Rogers,A.M., Borcherdt,R.D., Covington,P.A., and Perkins,D.M. (1984). A comparative ground response study near Los Angeles using recordings of Nevada nuclear tests and the 1971 San Fernando earthquake. Bull. Seism. Soc. Am. **74**, 1925-1949.

Rymer,M.J. (1987). The San Salvador earthquake of October 10, 1986 - Geological aspects. Earthquake Spectra, Vol.**3**, No.3, 436-462.

Shakal,A.F., Huang,M.J., Parke,D.L., and Linares,R. (1986). Summary of the processed strong-motion data, San Salvador earthquake of October 10, 1986. Proceedings from the San Salvador Earthquake Briefing, Nov.24, 1986, Washington D.C., U.S.A.

Singh, S.K., Lermo,J., Dominguez,T., Ordaz,M., Espinoza,J.M., Mena,E., and Quass,R. (1988). the Mexico earthquake of September 19, 1985: a study of amplification of seismic waves in the Valley of Mexico with respect to a hill zone site. Earthquake Spectra **4**, 653-673.

Schmidt-Thomé,M. (1975). The geology in the San Salvador area (El Salvador, Central America), a basis for city development and planning. Geologisches Jahrbuch, v.**13**, 207-228.

Şafak,E. (1991). Problems with using spectral ratios to estimate site amplification. Proc. Forth Int. Conf. on Seismic Zonation, Stanford, California, **II**, 277-284.

Weber, H.S., Weisemann,G., Lorenz,H., and Schmidt-Thomé,M. (1978). Mapa geológico de la República de El Salvador / América Central: Bundesanstalt für Geowissenschaften und Roshtoffe, Hannover, Germany, Scale: 1:100 000.

Weinberg,R.F. (1992). Neotectonic development of Western Nicaragua. Tectonics, Vol.**11**, No.5, 1010-1017.

Weisemann, G. (1975). Remarks on the geologic structure of the Republic of El Salvador, Central America: Mitteilungen Geologisch-Palaontologischen Institut, University of Hamburg, v.**44**, 557-574.

White,R.A., Harlow,D.H. and Alvarez,S. (1987). The San Salvador earthquake of October 10, 1986 - Seismological aspects and other recent local seismicity. Earthquake Spectra, Vol.**3**, No.3, 419-434.

FIGURE CAPTIONS:

Figure 1. The locations of the six accelerograph stations used in this study. At each site, the N-S component of the acceleration recordings from the October 10, 1986 earthquake are shown for comparison. Note the lower amplitudes at SHE. The major roads are shown for orientation.

Figure 2.a. Map showing the geology of the San Salvador area *(Simplified from the 1:15 000 geological map prepared by Centro de Investigaciones Geotécnicas, 1987).* Major fault trends, as well as the main roads are shown. **b.** The parallel N-S cross-sections, AA' AND BB', showing the lithology and thickness variations. The numbers at each site indicates the results from the penetrations tests.

Figure 3. The macroseismic intensity (Modified Mercalli) contour map *(from Alvarez, 1987).* The distribution of damage is also shown with darker patterns indicating higher damage *(modified from Centro de Investigaciones Geotécnicas, 1987).* The stars indicate the areas where total damage to buildings occurred. the epicenter of the October 10, 1986 earthquake is also shown by a larger star. Stippled line indicates the city limits. Note that the distribution is largely along a NNE-SSW trend.

Figure 4. The mainshock and the immediate aftershocks (within the first 24 hours) of the October 10, 1986 earthquake *(from White et al., 1987).* The first intermadiate aftershock (M_S=4.8) is shown on the northern part of the city. The focal mechanism of the main shock is shown on the lower left corner. The cross-section AA' clearly shows the steeply dipping fault plane.

Figure 5. The spectral plots and the spectral ratios of N-S components of the five sedimentary sites with respect to the bedrock reference site SHE. The solid lines are the spectras corresponding to the sedimentary sites, whereas the dashed lines indicate the spectra of the bedrock reference site. The acceleration traces for each site are also shown. All

amplitudes are in cm/sec^2. The accelerogram from SHE is shown on the right for comparison.

Figure 6. The spectral plots and the spectral ratios of E-W components of the five sedimentary sites with respect to the bedrock reference site SHE. Notations are as in Figure 5.

Figure 7. a. The maximum absolute accelerations (in g.) for the two horizontal components (N-S and E-W). Note that the SHE site has the lowest values. **b.** The maximum and average spectral amplification factors at different sedimentary sites with respect to the bedrock reference site for the N-S components. **c.** The maximum and average spectral amplification factors at different sedimentary sites with respect to the bedrock reference site for the E-W components.

Figure 8. a. The amplification factors at different critical frequencies that are common to all sites for the N-S components (see also *Table IV*). The upper left figure is the same data presented on a 3-D diagram. **b.** The amplification factors at different critical frequencies that are common to all sites for the E-W components (see also *Table IV*). The upper right figure is the same data presented on a 3-D diagram.

Figure 9. The spectral plots and the spectral ratios of four sedimentary sites N-S vs. vertical components. The IVU station is not included, because the vertical record is missing. In addition the bedrock reference site SHE is added for comparison. Note the relatively less amplifications at SHE. Both the N-S and the vertical accelerograms are also shown on the left of each spectral plot.

Figure 10. The spectral plots and the spectral ratios of four sedimentary sites E-W vs. vertical components. The IVU station is not included, because the vertical record is missing. In addition the bedrock reference site SHE is added for comparison. Note the relatively less amplifications at SHE. Both the E-W and the vertical accelerograms are also shown on the left of each spectral plot.

Figure 11. The comparison of the observed **(a)** and the synthetic **(b)** accelerograms for the three stations SHE, CIG and IGN. All traces are the N-S components. Note that the synthetic accelerograms indicate higher amplitudes at SHE with respect to CIG and IGN, which is the opposite of what is observed.

Table I. Site locations and the maximum accelerations *(Shakal et al., 1986)*.

			Max.Acceleration(g)			
Station	**Lat(°N)**	**Lon(°W)**	**N-S**	**E-W**	**Z**	**Distance(km)**
CIG	13.700	89.175	0.42	-0.71	0.40	4.3
IGN	13.714	89.171	0.40	-0.54	0.46	5.7
IVU	13.721	89.206	0.72	0.37	-----	5.3
UCA	13.683	89.237	-0.39	0.43	0.24	3.8
HCR	13.712	89.215	0.47	0.34	0.26	4.5
SHE	13.713	89.243	0.22	0.32	-0.15	6.2

Table II. Maximum and average amplification factors for different sites.

Station	Amplification Factor			
	N-S		E-W	
	Maximum	Average	Maximum	Average
CIG	15.0	4.1	6.0	3.1
IGN	22.0	6.1	6.5	2.9
IVU	14.0	3.1	8.0	3.9
UCA	7.8	3.3	4.6	3.4
HCR	17.0	5.2	4.6	1.4

Table III. Frequency band on which the amplification occurs

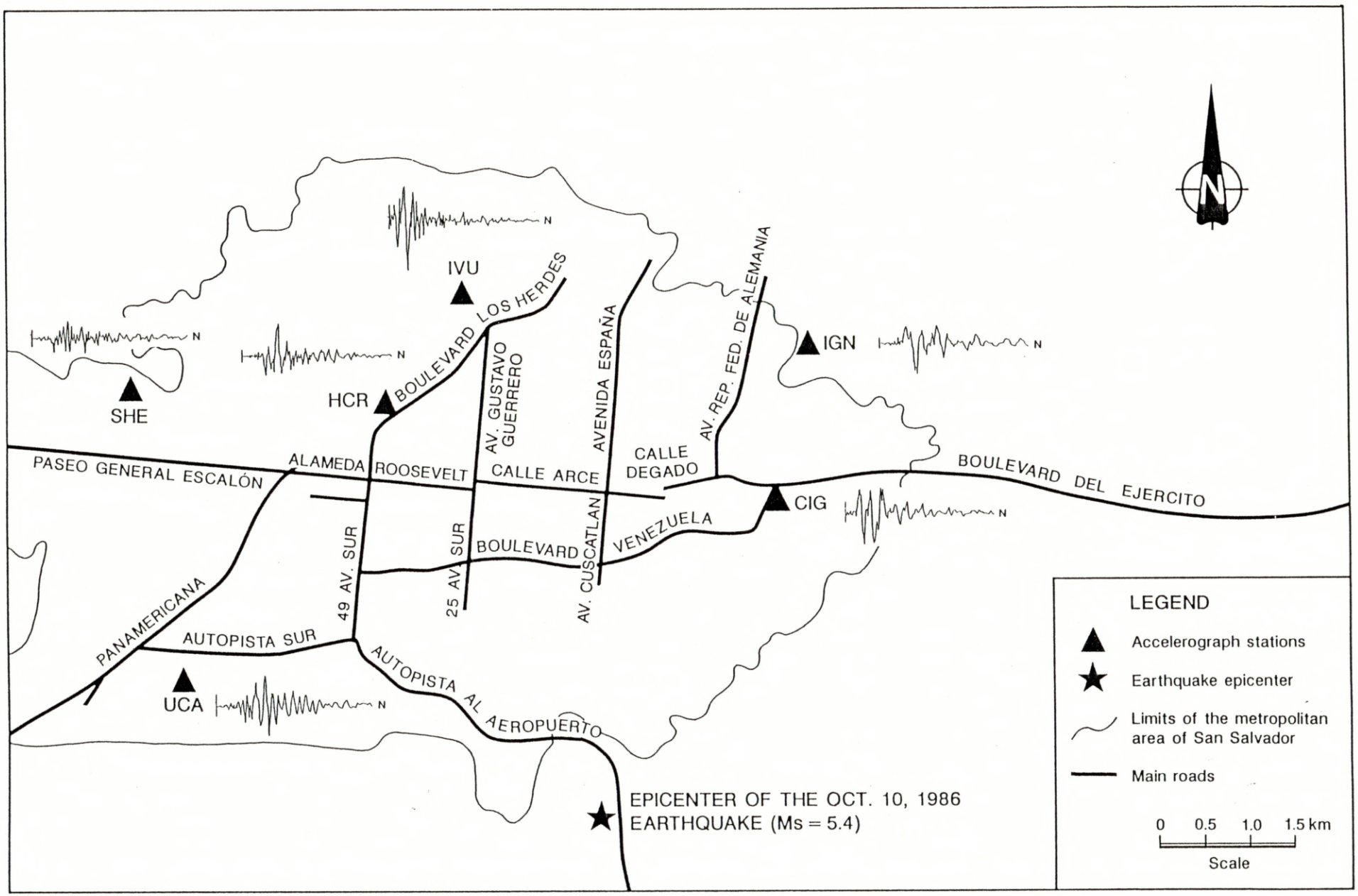
Station	Frequency band (Hz)	
	N-S	E-W
CIG	0.1 - 3.5	0.1 -10.0
IGN	0.1 - 2.3	0.1 - 3.0
IVU	0.5 - 3.2	0.1 - 0.8
UCA	0.3 - 3.3	0.1 - 2.9
HCR	0.2 - 2.5	----------

Table IV. Amplification factor at critical frequencies (common peaks).

Station	Amplification factor											
	0.4 Hz		0.7 Hz		1.3 Hz		2.0 Hz		2.3 Hz		3.0 Hz	
	NS	EW	NS	EW	NS	EW	NS	EW	NS	EW	NS	EW
CIG	2.1	5.1	6.8	5.4	15.	5.0	5.0	4.0	2.3	2.8	3.0	1.5
IGN	8.0	1.4	22.	6.0	8.0	6.5	5.0	3.0	1.0	4.2	1.1	1.0
IVU	0.9	1.3	6.0	3.4	14.	3.1	6.7	2.9	4.0	2.7	2.5	0.3
UCA	2.1	2.8	6.0	4.7	6.2	3.6	7.7	3.2	5.0	4.6	4.3	0.8
HCR	4.5	0.4	15.	3.0	8.0	3.1	6.7	4.3	1.0	3.7	1.9	0.5

Table V The crustal velocity model used in this study (Vp/Vs ratio is 1.78).

No. of layers	Depth to interface (km)	P-wave velocity (km/sec)
1	0.50	1.70
2	1.25	2.40
3	4.00	3.20
4	9.00	4.40
5	12.00	6.96
6	17.00	8.20


N
IVU
IGN
HCR
SHE
UCA
CIG
BOULEVARD LOS HEROES
AV. GUSTAVO GUERRERO
AVENIDA ESPAÑA
AV. REP. FED. DE ALEMANIA
PASEO GENERAL ESCALÓN
ALAMEDA ROOSEVELT
CALLE ARCE
CALLE DEGADO
BOULEVARD DEL EJERCITO
49 AV. SUR
25 AV. SUR
BOULEVARD VENEZUELA
AV. CUSCATLAN
PANAMERICANA
AUTOPISTA SUR
AUTOPISTA AL AEROPUERTO
EPICENTER OF THE OCT. 10, 1986
EARTHQUAKE (Ms = 5.4)
LEGEND
Accelerograph stations
Earthquake epicenter
Limits of the metropolitan area of San Salvador
Main roads
0 0.5 1.0 1.5 km
Scale

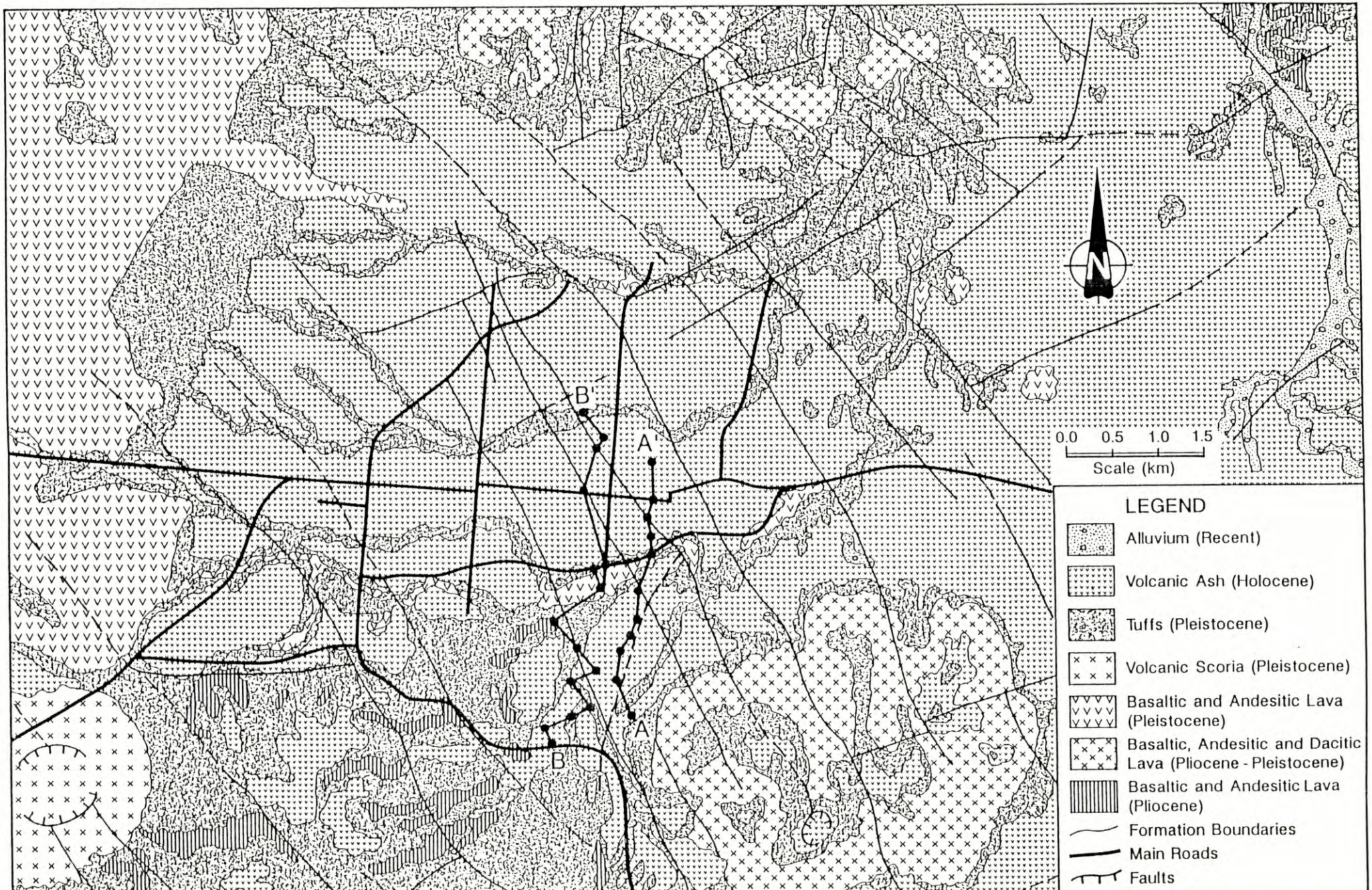
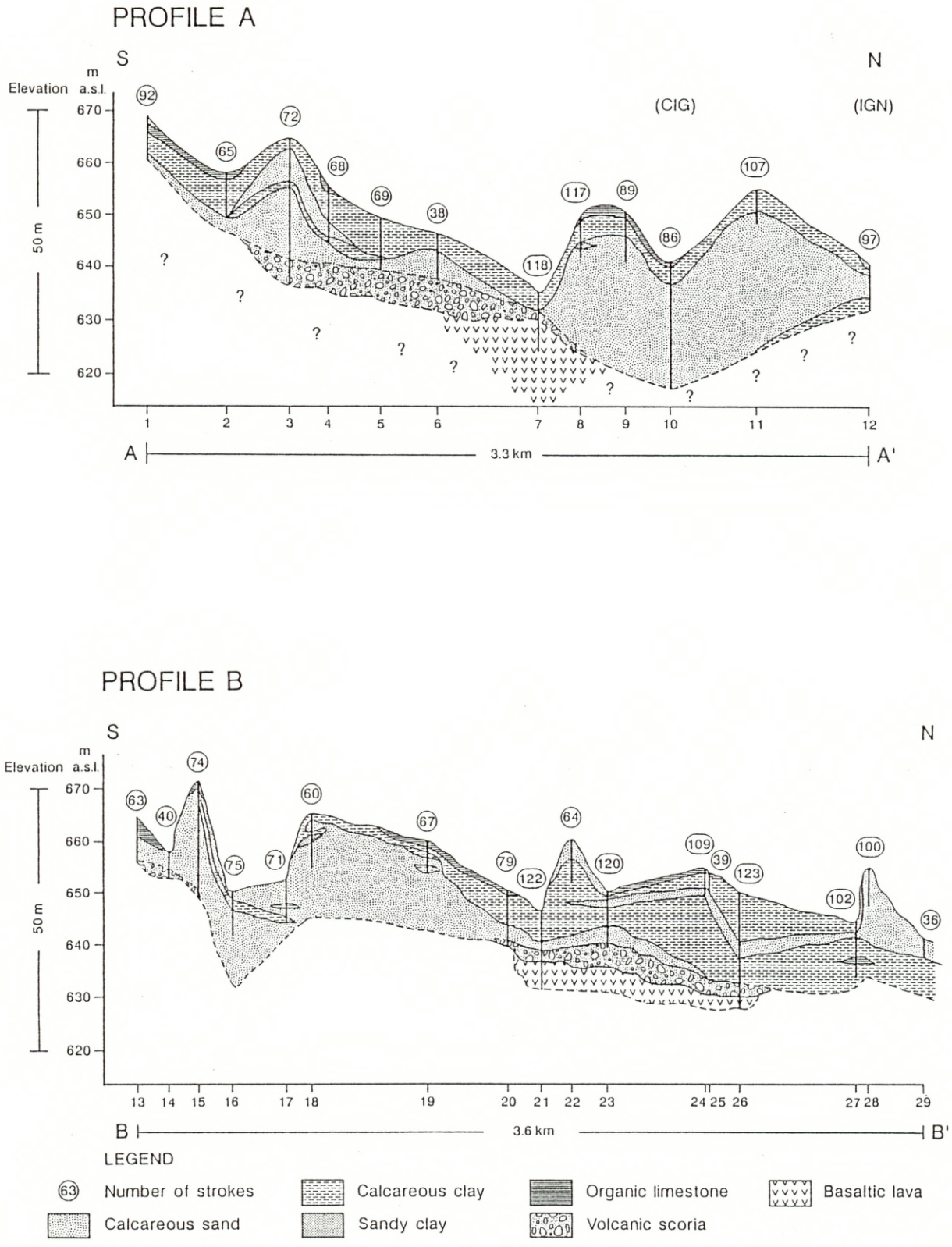

N
0.0 0.5 1.0 1.5
Scale (km)
LEGEND
Alluvium (Recent)
Volcanic Ash (Holocene)
Tuffs (Pleistocene)
Volcanic Scoria (Pleistocene)
Basaltic and Andesitic Lava (Pleistocene)
Basaltic, Andesitic and Dacitic Lava (Pliocene - Pleistocene)
Basaltic and Andesitic Lava (Pliocene)
Formation Boundaries
Main Roads
Faults
A
A'
B
B'

Figure 2. b.


PROFILE A
S
N
m
Elevation a.s.l.
(CIG)
(IGN)
50 m
670
660
650
640
630
620
92
72
65
68
69
38
118
117
89
86
107
97
1
2
3
4
5
6
7
8
9
10
11
12
A
3.3 km
A'
PROFILE B
S
N
m
Elevation a.s.l.
50 m
670
660
650
640
630
620
74
63
40
60
75
71
67
64
79
122
120
109
39
123
100
102
36
13
14
15
16
17
18
19
20
21
22
23
24
25
26
27
28
29
B
3.6 km
B'
LEGEND
63 Number of strokes
Calcareous sand
Calcareous clay
Sandy clay
Organic limestone
Volcanic scoria
Basaltic lava

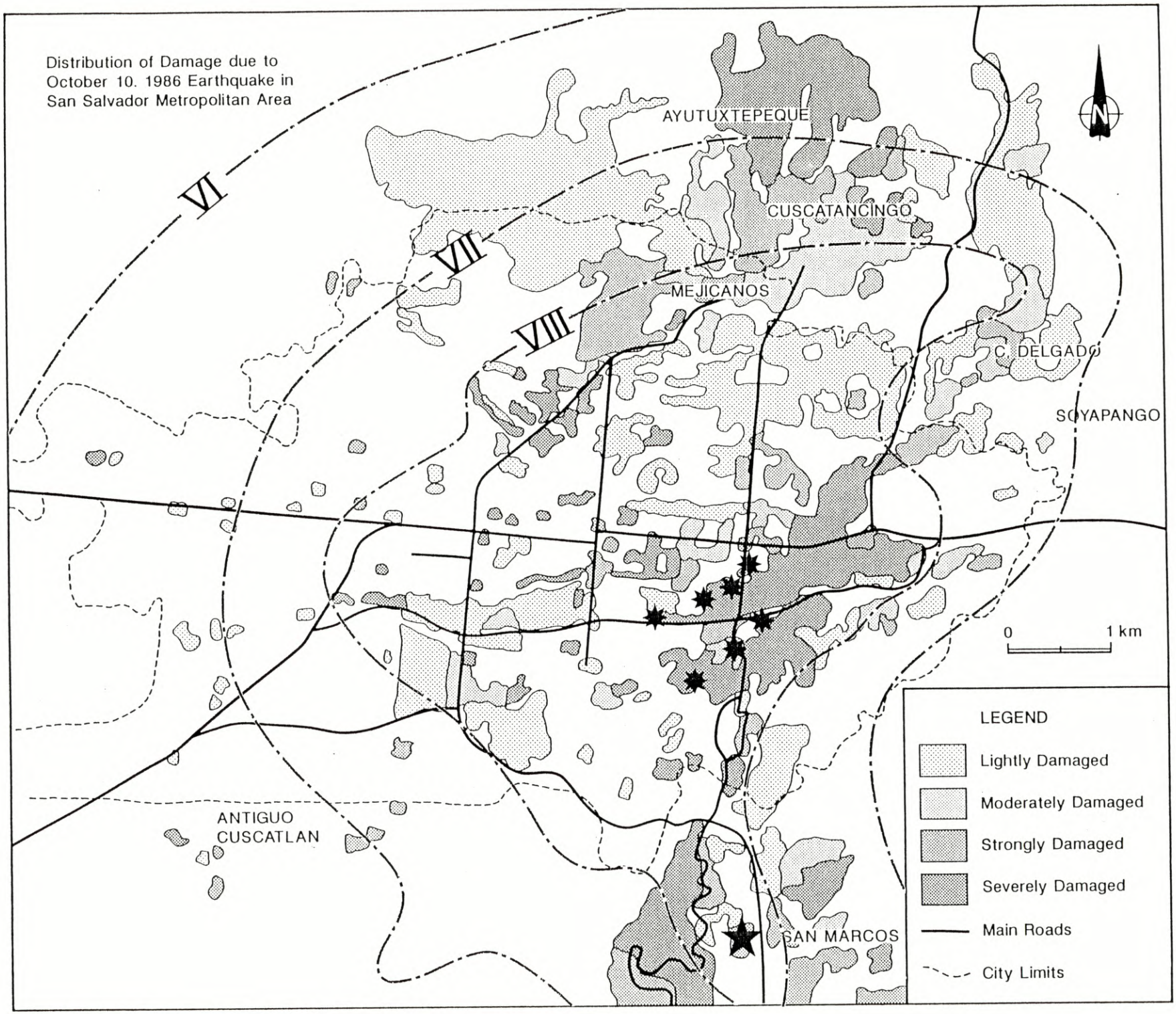
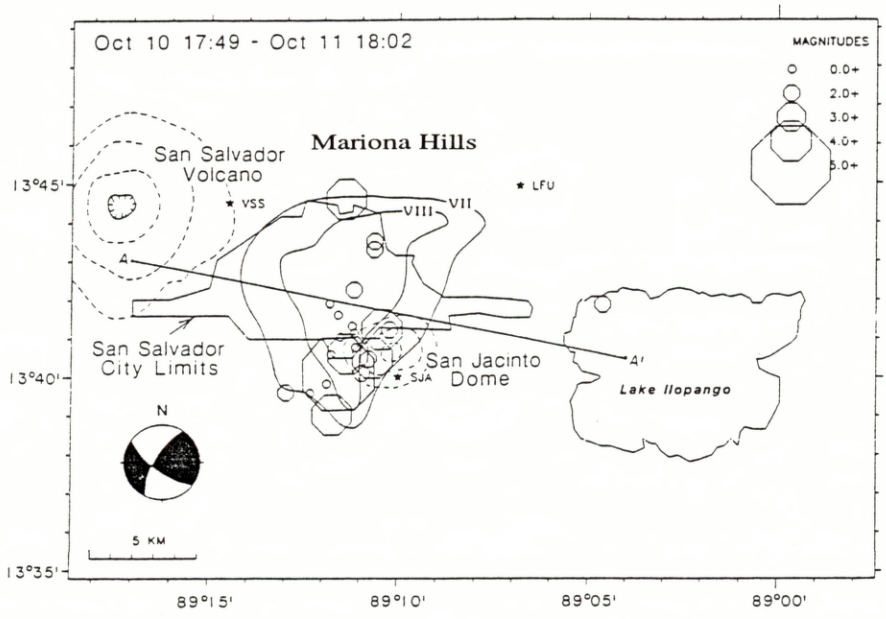

Distribution of Damage due to
October 10. 1986 Earthquake in
San Salvador Metropolitan Area
AYUTUXTEPEQUE
CUSCATANCINGO
MEJICANOS
C. DELGADO
SOYAPANGO
ANTIGUO
CUSCATLAN
SAN MARCOS
VI
VII
VIII
N
0
1 km
LEGEND
Lightly Damaged
Moderately Damaged
Strongly Damaged
Severely Damaged
Main Roads
City Limits

Figure 3.

Figure 4.


Oct 10 17:49 - Oct 11 18:02
MAGNITUDES
0.0+
2.0+
3.0+
4.0+
5.0+
Mariona Hills
San Salvador Volcano
VSS
LFU
VIII
VII
A
A'
San Salvador City Limits
San Jacinto Dome
SJA
Lake Ilopango
N
5 KM
13°45'
13°40'
13°35'
89°15'
89°10'
89°05'
89°00'

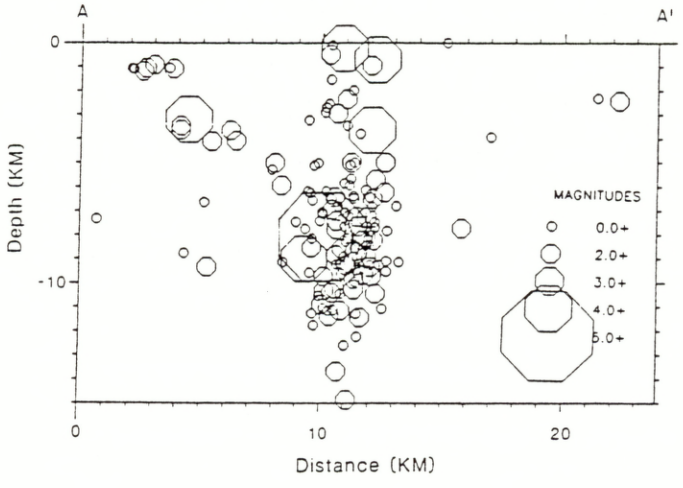

A
A'
0
-10
Depth (KM)
MAGNITUDES
0.0+
2.0+
3.0+
4.0+
5.0+
0
10
20
Distance (KM)

Figure 5.

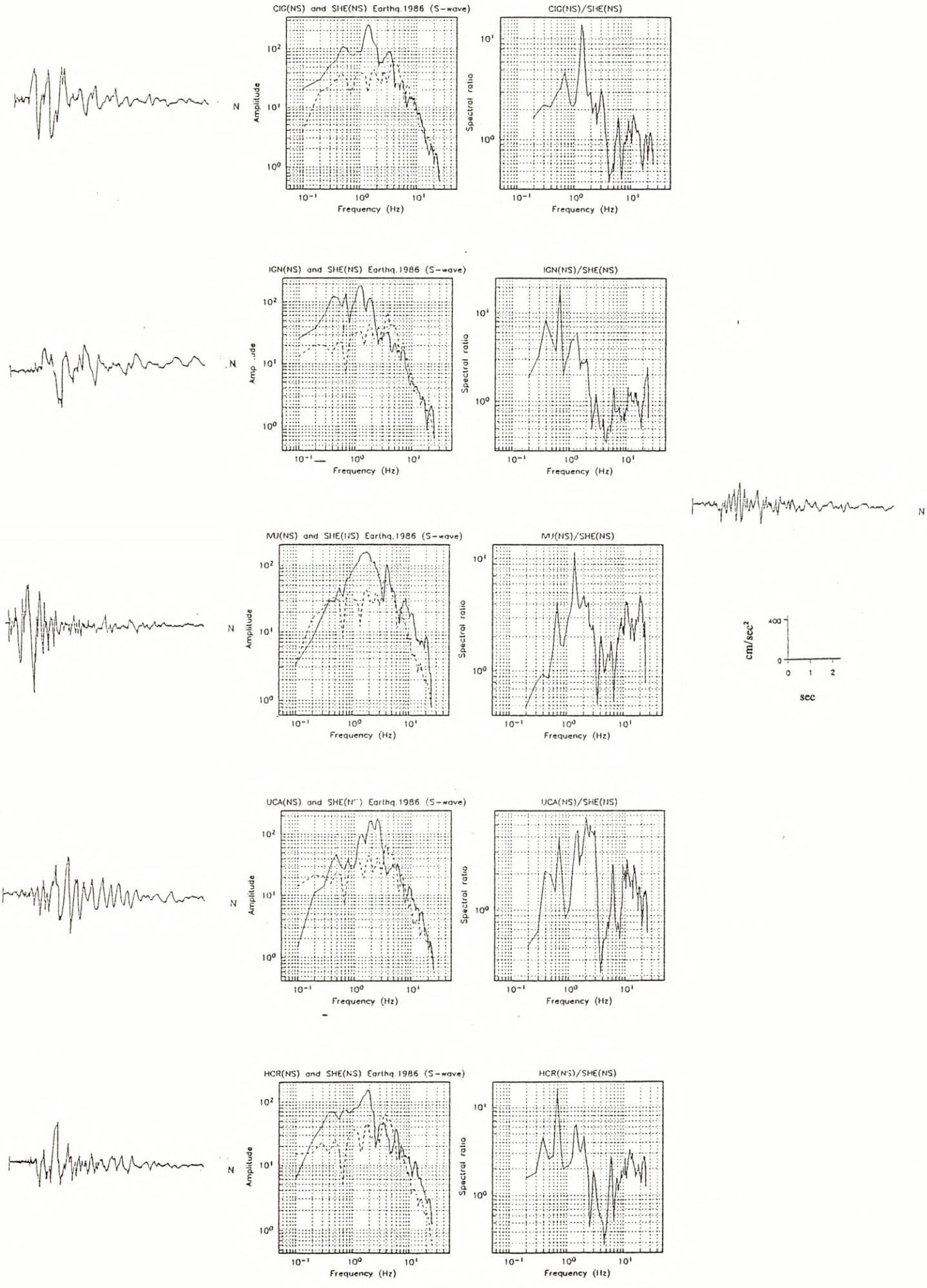

CIG(NS) and SHE(NS) Earthq.1986 (S-wave)
CIG(NS)/SHE(NS)
IGN(NS) and SHE(NS) Earthq.1986 (S-wave)
IGN(NS)/SHE(NS)
MJI(NS) and SHE(NS) Earthq.1986 (S-wave)
MJI(NS)/SHE(NS)
UCA(NS) and SHE(NS) Earthq.1986 (S-wave)
UCA(NS)/SHE(NS)
HCR(NS) and SHE(NS) Earthq.1986 (S-wave)
HCR(NS)/SHE(NS)
Amplitude
Spectral ratio
Frequency (Hz)
N
cm/sec²
400
0
0 1 2
sec

Figure 6.

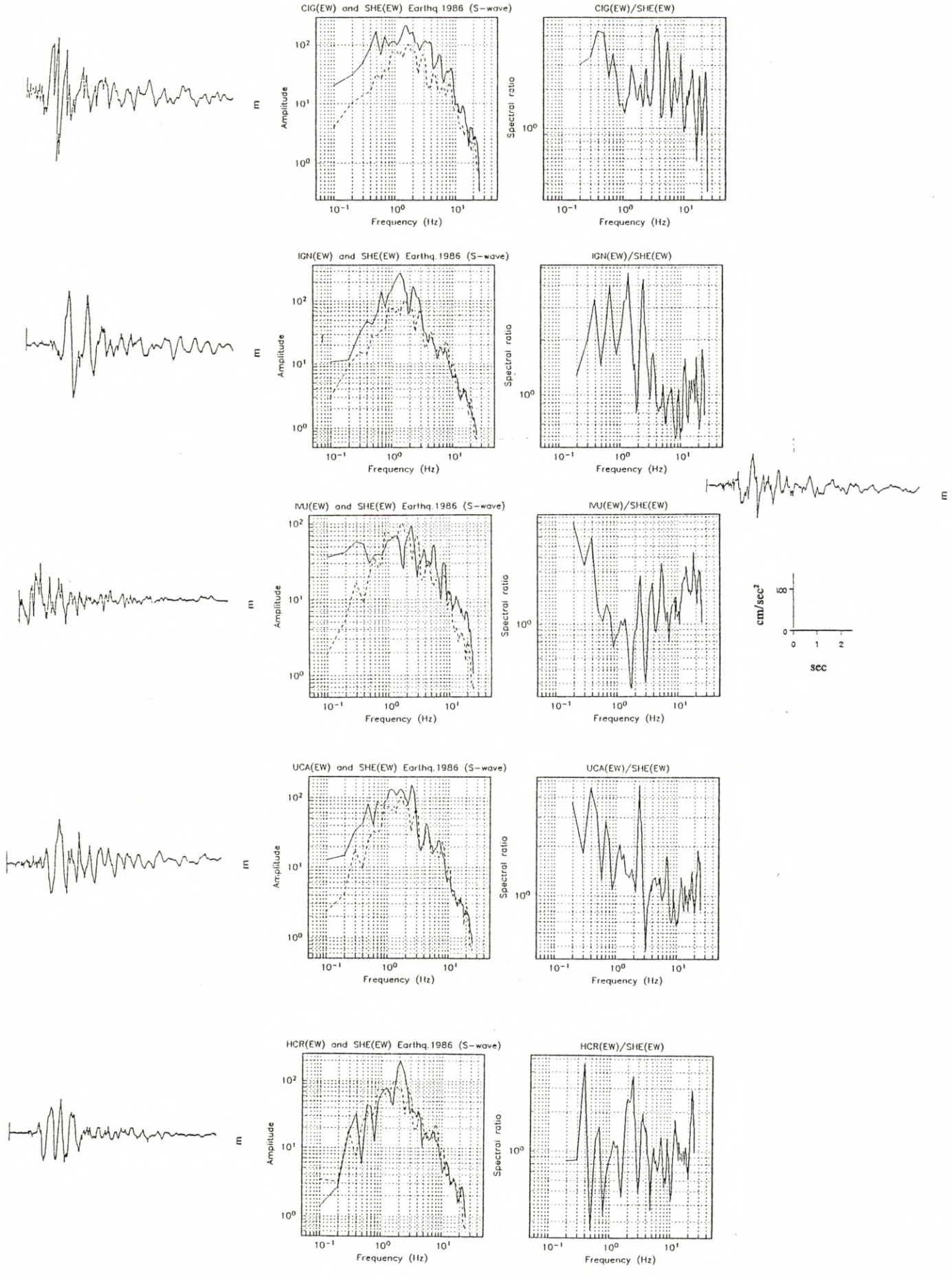
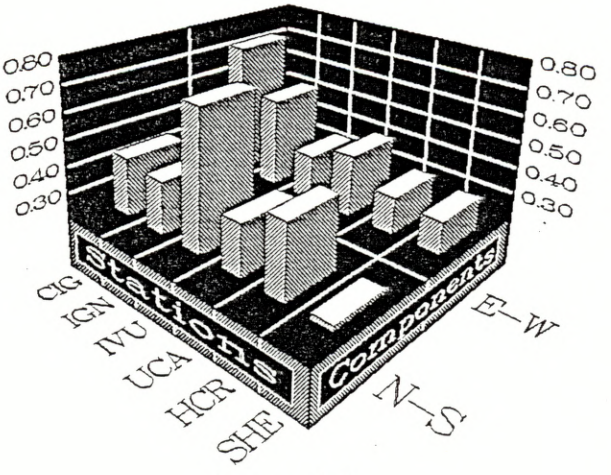

CIG(EW) and SHE(EW) Earthq.1986 (S-wave)
CIG(EW)/SHE(EW)
IGN(EW) and SHE(EW) Earthq.1986 (S-wave)
IGN(EW)/SHE(EW)
IVU(EW) and SHE(EW) Earthq.1986 (S-wave)
IVU(EW)/SHE(EW)
UCA(EW) and SHE(EW) Earthq.1986 (S-wave)
UCA(EW)/SHE(EW)
HCR(EW) and SHE(EW) Earthq.1986 (S-wave)
HCR(EW)/SHE(EW)
Amplitude
Spectral ratio
Frequency (Hz)
cm/sec²
sec

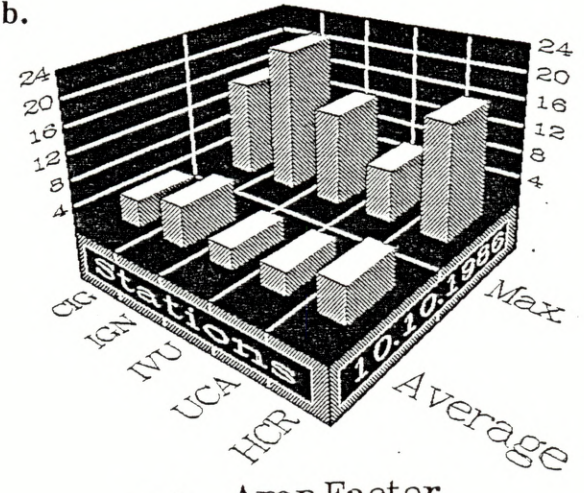
Figure 7.

a.



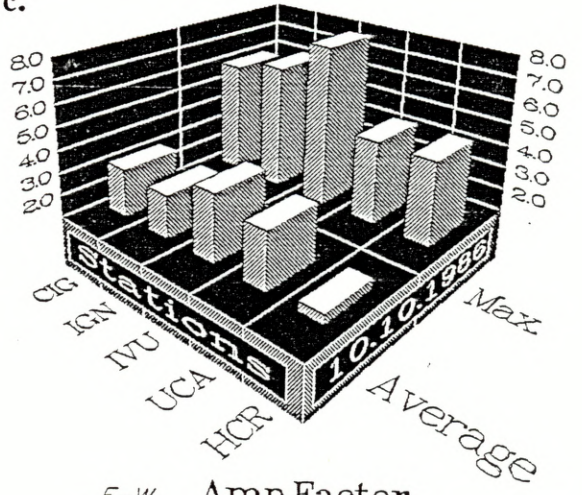
Amax(g)

b.



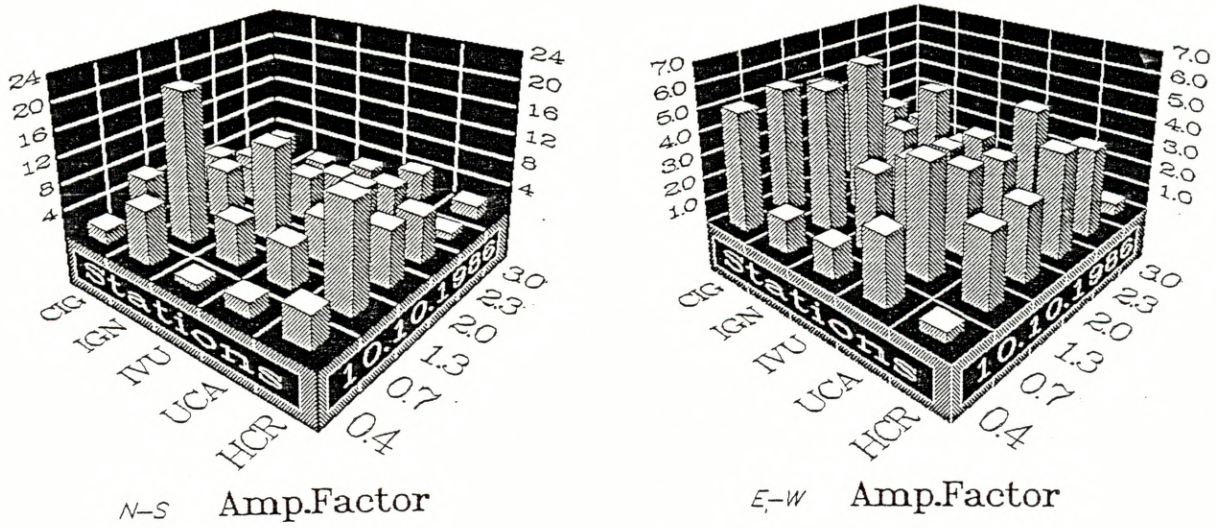
N–S Amp.Factor

c.

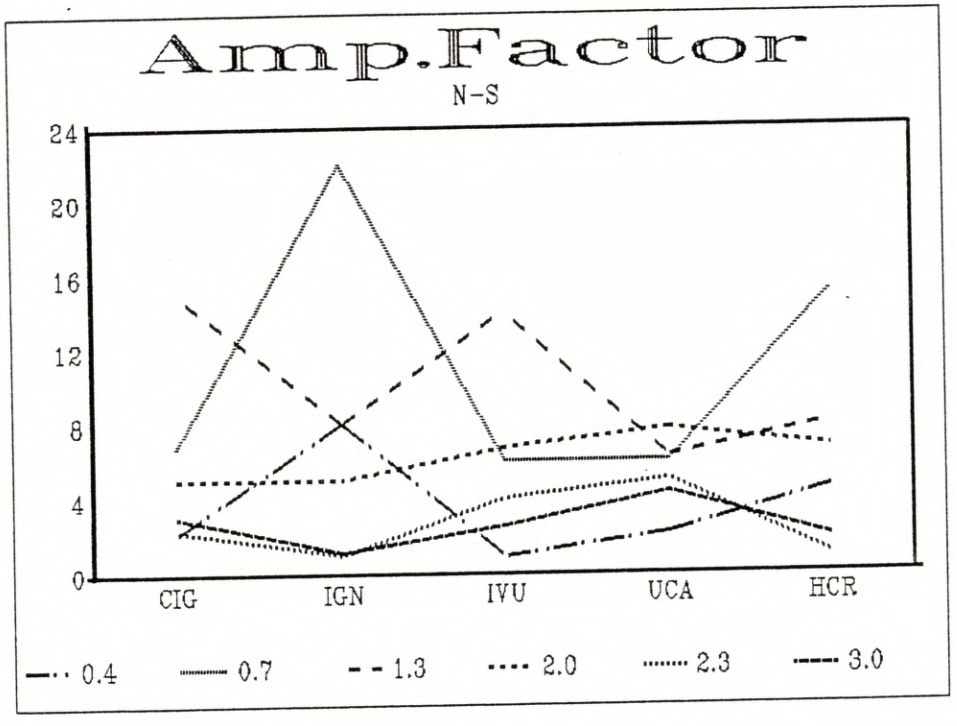


E–W Amp.Factor

Figure 8.


24
20
16
12
8
4
Stations
10.10.1986
CIG
IGN
IVU
UCA
HCR
0.4
0.7
1.3
2.0
2.3
3.0
N-S Amp.Factor
7.0
6.0
5.0
4.0
3.0
2.0
1.0
E-W Amp.Factor

a.


Amp.Factor
N-S
24
20
16
12
8
4
0
CIG
IGN
IVU
UCA
HCR
0.4
0.7
1.3
2.0
2.3
3.0

b.

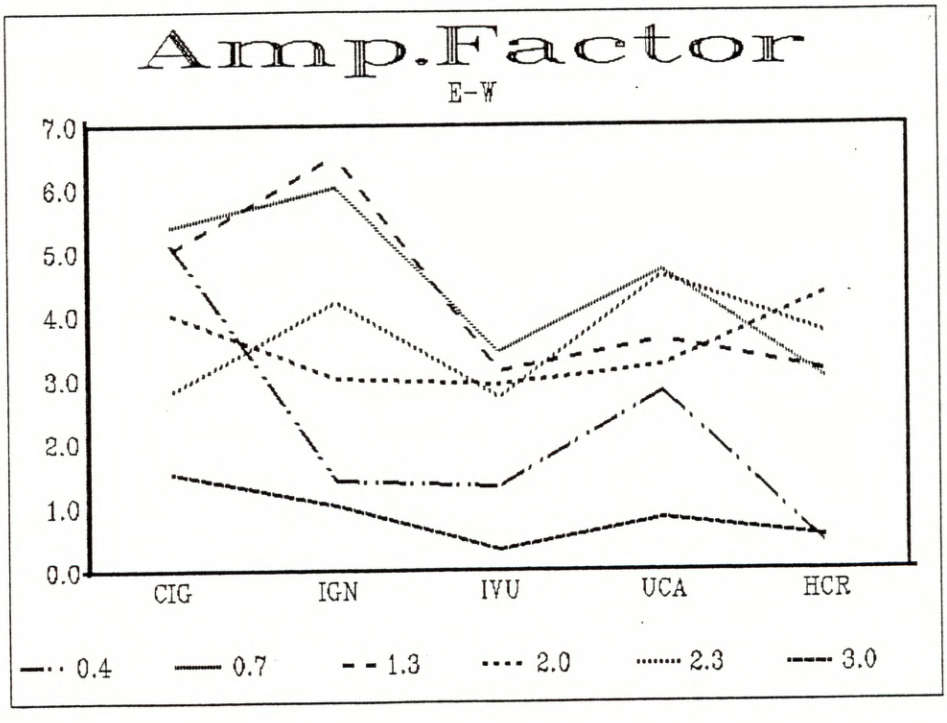

Amp.Factor
E-W
7.0
6.0
5.0
4.0
3.0
2.0
1.0
0.0
CIG
IGN
IVU
UCA
HCR
0.4
0.7
1.3
2.0
2.3
3.0

Figure 9.

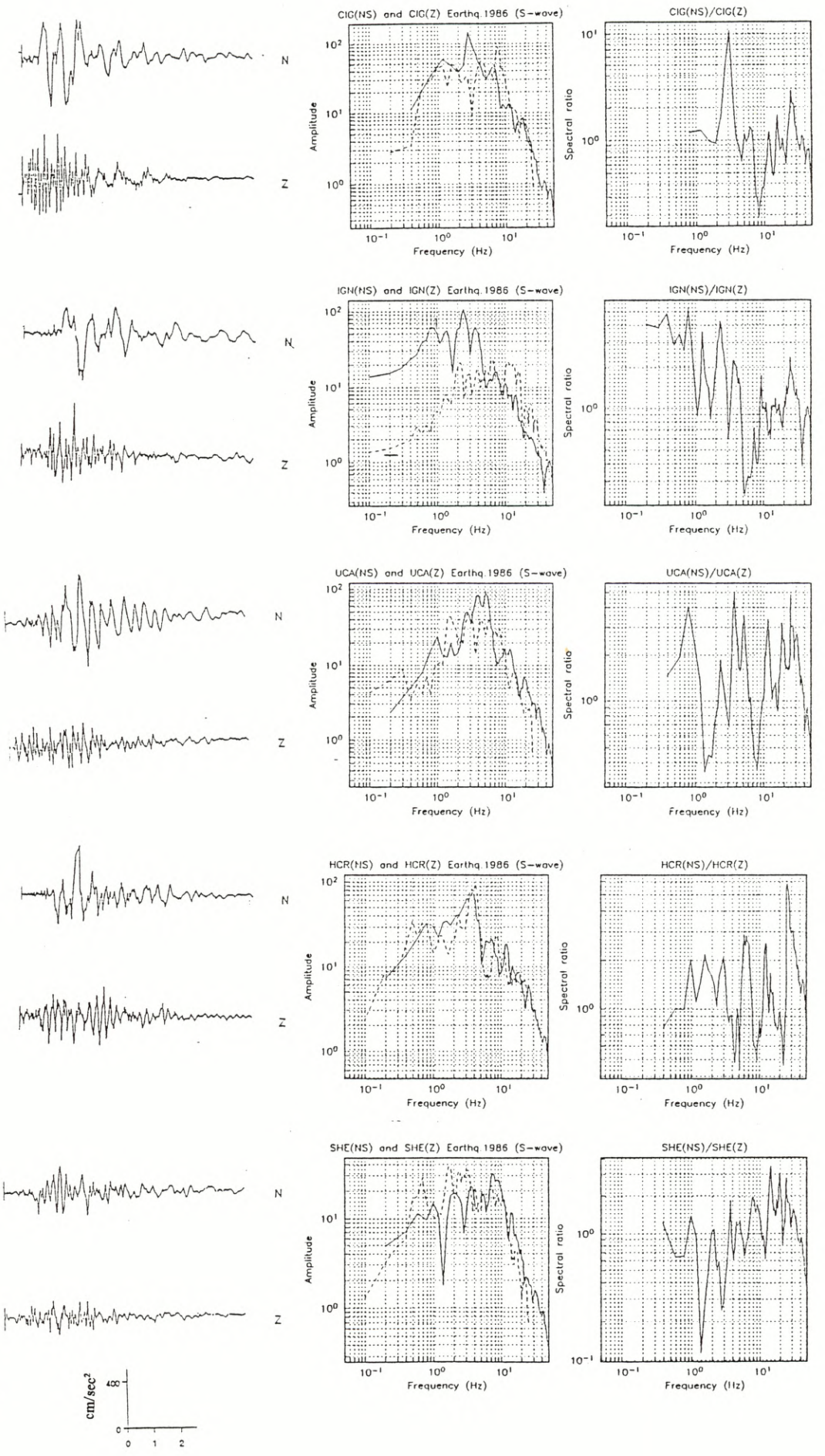
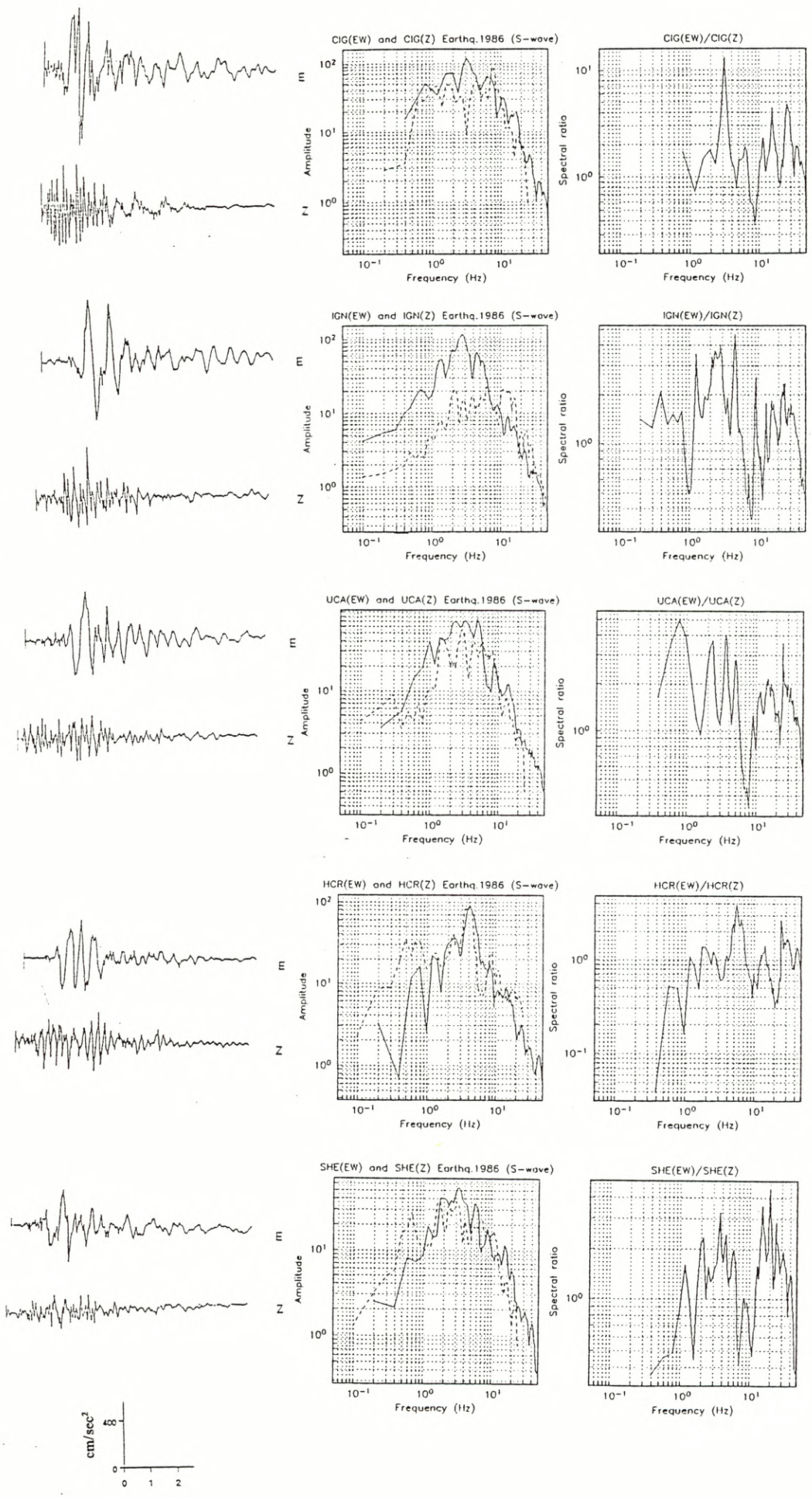

CIG(NS) and CIG(Z) Earthq.1986 (S-wave)
CIG(NS)/CIG(Z)
IGN(NS) and IGN(Z) Earthq.1986 (S-wave)
IGN(NS)/IGN(Z)
UCA(NS) and UCA(Z) Earthq.1986 (S-wave)
UCA(NS)/UCA(Z)
HCR(NS) and HCR(Z) Earthq.1986 (S-wave)
HCR(NS)/HCR(Z)
SHE(NS) and SHE(Z) Earthq.1986 (S-wave)
SHE(NS)/SHE(Z)
N
Z
Amplitude
Spectral ratio
Frequency (Hz)
cm/sec²
400
0
0 1 2
sec

Figure 10.


CIG(EW) and CIG(Z) Earthq.1986 (S-wave)
CIG(EW)/CIG(Z)
IGN(EW) and IGN(Z) Earthq.1986 (S-wave)
IGN(EW)/IGN(Z)
UCA(EW) and UCA(Z) Earthq.1986 (S-wave)
UCA(EW)/UCA(Z)
HCR(EW) and HCR(Z) Earthq.1986 (S-wave)
HCR(EW)/HCR(Z)
SHE(EW) and SHE(Z) Earthq.1986 (S-wave)
SHE(EW)/SHE(Z)
E
N
Z
Amplitude
Spectral ratio
Frequency (Hz)
cm/sec²
400
0
0
1
2
sec

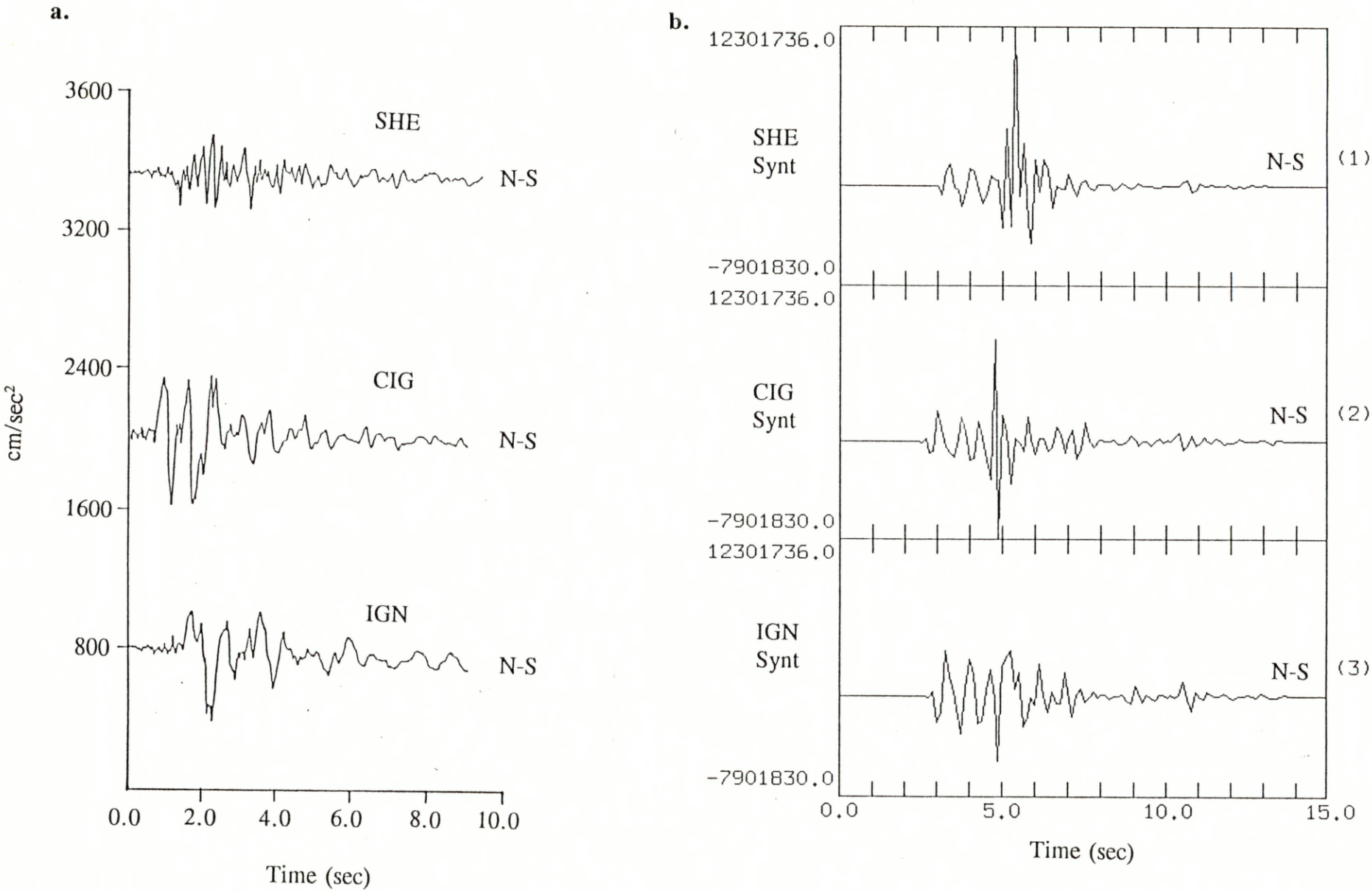

a.
3600
3200
2400
1600
800
cm/sec²
SHE
N-S
CIG
N-S
IGN
N-S
0.0
2.0
4.0
6.0
8.0
10.0
Time (sec)
b.
12301736.0
SHE
Synt
N-S
(1)
-7901830.0
12301736.0
CIG
Synt
N-S
(2)
-7901830.0
12301736.0
IGN
Synt
N-S
(3)
-7901830.0
0.0
5.0
10.0
15.0
Time (sec)

Figure 11.